A New Series of Homoleptic, Paramagnetic Organochromium Derivatives: Synthesis, Characterization, and Study of Their Magnetic Properties

Pablo J. Alonso, Juan Forniés,* María Angeles García-Monforte, Antonio Martín, Babil Menjón, and Conrado Rillo[a]

Abstract: The synthesis and characterization of the triad of organochromium derivatives $[Cr(C_6Cl_5)_4]^{n-}$ ($n = 0$, 1, 2) are described. By treating $[CrCl_3(thf)_3]$ with LiC_6Cl_5 in 1:5 molar ratio, the salt $[Li(thf)_4][Cr^{III}(C_6Cl_5)_4]$ (**1**) was obtained as a violet solid in 57% yield. Oxidation of **1** with $[N(4\text{-}BrC_6H_4)_3][SbCl_6]$ yielded the neutral complex $[Cr^{IV}(C_6Cl_5)_4]$ (**2**) as a brown solid in 71% yield. The arylation of $[CrCl_2(thf)]$ with LiC_6Cl_5 under similar conditions as above gave $[\{Li(thf)_3\}_2(\mu\text{-}Cl)]_2[Cr^{II}(C_6Cl_5)_4]$ (**3**) as an extremely air- and water-sensitive red solid in 47% yield. The crystal and molecular structures of **1** and **3** have been established by X-ray diffraction methods. Complex **3** contains the unusual cation $[\{Li(thf)_3\}_2(\mu\text{-}Cl)]^+$ with an almost linear Li-Cl-Li unit (174.2(6)°). All four C_6Cl_5 groups are σ-bonded to the Cr^{II} center, which is located in a square-planar environment. The local geometry around the Cr^{III} center in **1** is, in turn, pseudo-octahedral, since two of the C_6Cl_5 groups act as standard σ-bonded monodentate ligands, while the other two act as small-bite didentate ligands coordinated through both the *ipso*-C and one of the *ortho*-Cl atoms. Compounds **1**–**3** are paramagnetic with maximum spin multiplicity each (EPR and magnetization measurements).

Keywords: chromium · cyclic voltammetry · EPR spectroscopy · homoleptic compounds · magnetic properties · organochromium compounds

Introduction

The preparation of organochromium derivatives and the study of their properties have attracted the chemist's interest during virtually the whole 20th century.[1–12] For many years, chromium was believed to be the only transition metal for which sufficiently stable σ-aryl derivatives could be isolated.[2, 3] Those enigmatic species, however, turned out to be (π-arene)chromium compounds and thus the question on the stability of (σ-organyl)–transition-metal bonds re-emerged.[4–6] Since then, the organometallic chemistry of chromium has been dominated chiefly by systems containing unsaturated organic moieties π-coordinated to low-valent chromium centers as is, for instance, the case of the plethora of half-sandwich derivatives with formula $[Cr(\pi\text{-arene})(CO)_3]$.[7] In contrast, only a handful of homoleptic (i.e., not bearing additional stabilizing ligands)[8] (σ-organyl)chromium derivatives have been prepared to date.[9] Meanwhile, a number of chromium compounds have been found to be useful reagents in advanced organic synthesis, particularly in processes giving rise to C–C bond formation.[10] Moreover, both homogeneous and heterogeneous chromium-based catalysts have been developed for the polymerization of terminal alkenes.[11] It is currently accepted that all these processes necessarily involve (σ-organyl)chromium species in intermediate oxidation states (II / III / IV) at key steps in the reaction pathways. These species, however, are not very amenable to study because, in the absence of any metal-metal bond, they should be paramagnetic, which implies the use of EPR as the tool of choice in order to gain more detailed insight into their nature.

Further to a previous communication,[12] we report now on the synthesis and characterization of a highly unusual series of homoleptic, paramagnetic (σ-organyl)chromium derivatives with the formulae $[Cr(C_6Cl_5)_4]^{n-}$ ($n = 0$, 1, 2), containing chromium in oxidation states IV, III, and II, respectively.

[a] Prof. Dr. J. Forniés, Prof. Dr. P. J. Alonso, Dipl.-Chem. M. A. García-Monforte, Dr. A. Martín, Dr. B. Menjón, Prof. Dr. C. Rillo
Instituto de Ciencia de Materiales de Aragón
Facultad de Ciencias, Universidad de Zaragoza-C.S.I.C.
Pza. S. Francisco s/n, 50009 Zaragoza (Spain)
Fax: (+34) 976761187
E-mail: forniesj@posta.unizar.es

Supporting information for this article is available on the WWW under http://www.chemeurj.org/ or from the author. Detailed derivation of the polynomial expression of $\chi(T)$ given in Equation (2) and graphical representation of $T\chi(T)$ vs T for compounds **1**–**3** (PDF).

Results and Discussion

Synthesis and structural characterization of 1: The reaction of $[CrCl_3(thf)_3]$ with LiC_6Cl_5 in 1:5 molar ratio and subsequent treatment gives $[Li(thf)_4][Cr^{III}(C_6Cl_5)_4]$ (**1**) in 57% yield as a

 © 2002 WILEY-VCH Verlag GmbH & Co. KGaA, Weinheim 0947-6539/02/0817-4056 $ 20.00+.50/0 *Chem. Eur. J.* **2002**, *8*, No. 17

violet solid (Scheme 1). This compound is air- and moisture-sensitive and has a limited thermal stability. This tendency to decompose is in keeping with previous reports on (σ-aryl)chromium(III) compounds, which are known to rearrange in the absence of stabilizing ligands, eventually yielding

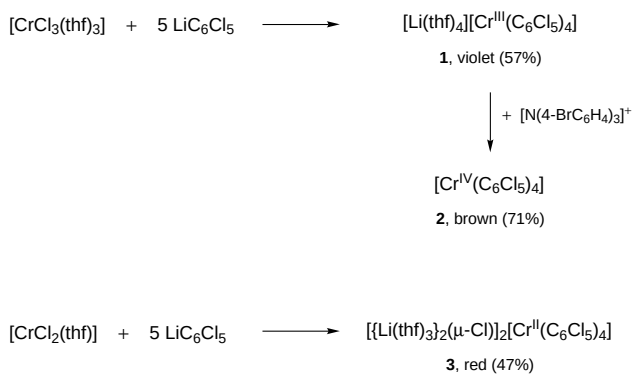

Scheme 1.

π-arene compounds of low-valent chromium.[13] As far as we know, there are only a few homoleptic organochromium(III) compounds with general formula $[CrR_n]^{(n-3)-}$, in which R is an organyl group and $n = 6-3$. In the hexaorganyl compounds $[Li(Et_2O)]_3[CrPh_6]$[14] and $[Li(1,4\text{-dioxane})]_3[CrMe_6]$[15] the chromium atom has been found to be in almost octahedral environments—the preferred geometry in chromium(III) chemistry.[16] On the other hand, the five phenyl groups in $Na_2[CrPh_5] \cdot 3\,Et_2O \cdot THF$ are arranged in a distorted trigonal bipyramidal geometry.[17] Remarkably, non-planar, three-coordinate chromium has been found in the single example of triorganylchromium: $[Cr\{CH(SiMe_3)_2\}_3]$.[18] However, no structural information is available for the only known tetraorganylchromate species: $Li[Cr(2\text{-}OMeC_6H_4)_4] \cdot Et_2O$[19] and $Li[Cr(2,4,6\text{-}Me_3C_6H_2)_4] \cdot 4\,THF$.[20] In the former, the phenyl group bears the 2-methoxyphenyl substituent, which enables the whole ligand to act as a chelate; thus, the chromium atom easily achieves a six-coordinate environment. The structure of the latter $[CrR_4]^-$ species is more intriguing, since it contains only four mesityl groups, which cannot act as standard chelate ligands. Unfortunately, the role of the potentially coordinating solvent molecules remains unclear in both cases. In this context, it is interesting to note the critical effect of the solvent on the stability of the unsubstituted tetraphenylchromate(III) salts $M[CrPh_4]$ (M = Li or Na): while they could not even be isolated from solutions in Et_2O or THF, the use of 1,2-dimethoxyethane (DME) allowed to obtain the compounds $M[CrPh_4] \cdot 4\,DME$. On the basis of thermolytic studies, Hein and Schmiedeknecht concluded, however, that these compounds were not homoleptic species but instead solvent-stabilized derivatives with formula $M[CrPh_4 \cdot 2dme] \cdot 2\,DME$.[21]

We succeeded in obtaining suitable crystals of the solvate $\mathbf{1} \cdot 0.5\,Et_2O \cdot 0.5\,C_6H_{14}$ for X-ray diffraction analysis. As far as we know, this is the first structural characterization of a homoleptic tetraorganylchromate(III) salt. Selected interatomic distances and angles are gathered in Table 1. The structure confirms that the anion $[Cr^{III}(C_6Cl_5)_4]^-$ contains four Cr–C σ bonds (Figure 1). However, the tendency of the chromium(III) ion to achieve an octahedral environment is so pronounced that two additional intramolecular Cr–Cl interactions are formed. Thus, two of the C_6Cl_5 groups act as monodentate σ-bonded ligands, while the other two act as chelating ligands through their *ipso*-C and one of the *o*-Cl atoms. The formation of such *o*-Cl – Cr interactions does not involve any significant lengthening in the related $C_o - Cl_o$ bonds, which are similar to the rest of the C – Cl distances. Nevertheless, the interaction of one of the *o*-Cl atoms with the metal entails a swing of the corresponding aryl ring as evidenced by a) the different $Cr\text{-}C_{ipso}\text{-}C_o$ angles observed (ring 1: Cr-C(1)-C(2) 112.4(9)°, Cr-C(1)-C(6) 133.3(8)°; ring 2: Cr-C(7)-C(12) 109.4(7)°, Cr-C(7)-C(8) 136.7(8)°) and b) the lengthening of the Cr···Cl distance with the non-interacting *o*-Cl atom on the same ring (ring 1: Cr–Cl(2) 300.1(4) vs Cr···Cl(6) 376.2(4) pm; ring 2: Cr–Cl(12) 281.8(3) vs Cr···Cl(8) 382.2(3) pm). Ring 3 can be considered as an internal structural reference for a typical monodentate C_6Cl_5 ligand, since its two *o*-Cl atoms are almost equidistant from the Cr center (Cr···Cl(14) 338.7(3) and Cr···Cl(18) 340.6(4) pm) and the two $Cr\text{-}C_{ipso}\text{-}C_o$ angles are virtually identical (Cr-C(13)-C(14) 123.8(8)° and Cr-C(13)-C(18) 122.5(8)°). Although we consider ring 4 as a monodentate ligand because of the very long Cr···Cl distances (Cr···Cl(20) 321.9(4) and Cr···Cl(24) 361.3(4) pm) it is also moderately swung (Cr-C(19)-C(20) 116.1(8)° and Cr-C(19)-C(24) 128.8(9)°).

The pentachlorophenyl group should arguably be a very poor chelating ligand considering the following: 1) the low general tendency of halocarbons to be coordinated,[22] 2) the

Abstract in Spanish: *En este trabajo se describe la síntesis y caracterización de la tríada de organoderivados de Cr de fórmula $[Cr(C_6Cl_5)_4]^{n-}$ (n = 0, 1, 2). El tratamiento de $[CrCl_3(thf)_3]$ con LiC_6Cl_5 en proporción molar 1:5 permite obtener $[Li(thf)_4][Cr^{III}(C_6Cl_5)_4]$ (**1**) en forma de un sólido violeta (57% de rendimiento). La oxidación de **1** con $[N(4\text{-}BrC_6H_4)_3][SbCl_6]$ da lugar a la especie neutra $[Cr^{IV}(C_6Cl_5)_4]$ (**2**), que se aísla con un 71% en forma de un sólido marrón. Por arilación de $[CrCl_2(thf)]$ con LiC_6Cl_5 en condiciones similares a las anteriormente descritas, se obtiene $[\{Li(thf)_3\}_2(\mu\text{-}Cl)]_2[Cr^{II}(C_6Cl_5)_4]$ (**3**) en forma de un sólido rojo extremadamente sensible al aire y a la humedad (47% de rendimiento). Las estructuras de los compuestos **1** y **3** se han determinado mediante difracción de rayos X. El catión del compuesto **3**, $[\{Li(thf)_3\}_2(\mu\text{-}Cl)]^+$, es raro y tiene una disposición Li-Cl-Li casi lineal (174.2(6)°). El Cr^{II} en el anión de **3** está situado en un entorno cuadrado plano definido por los cuatro grupos $\sigma\text{-}C_6Cl_5$. Por su parte, la geometría local del Cr^{III} en **1** puede describirse como pseudo-octaédrica ya que, mientras dos de los grupos C_6Cl_5 actúan como ligandos monodentados de tipo σ, los otros dos actúan como ligandos didentados a través de los átomos ipso-C y uno de los ortho-Cl. Los compuestos **1**–**3** son paramagnéticos con multiplicidad de spin máxima en cada caso (medidas de magnetización y de EPR).*

 © 2002 WILEY-VCH Verlag GmbH & Co. KGaA, Weinheim 0947-6539/02/0817-4057 $ 20.00+.50/0

Table 1. Selected interatomic distances [pm] and angles [°] for $\mathbf{1}\cdot 0.5\,Et_2O\cdot 0.5\,C_6H_{14}$.[a]

Ring 1		Ring 2	
Cr−C(1)	213.7(11)	Cr−C(7)	207.3(10)
Cr−Cl(2)	300.1 (4)	Cr···Cl(8)	382.2 (3)
Cr···l(6)	376.2 (4)	Cr−Cl(12)	281.8 (3)
C(1)−C(2)	139.0(15)	C(7)−C(8)	141.0(14)
C(1)−C(6)	142(2)	C(7)−C(12)	138.5(13)
C(2)−Cl(2)	174.1(12)	C(8)−Cl(8)	173.8(10)
C(6)−Cl(6)	172.3(12)	C(12)−Cl(12)	174.9(10)
Cr-C(1)-C(2)	112.4(9)	Cr-C(7)-C(8)	136.7(8)
Cr-C(1)-C(6)	133.3(8)	Cr-C(7)-C(12)	109.4(7)
C(2)-C(1)-C(6)	113.5(10)	C(8)-C(7)-C(12)	113.8(9)
Ring 3		Ring 4	
Cr−C(13)	208.1(10)	Cr−C(19)	217.3(11)
Cr···Cl(14)	338.7 (3)	Cr···Cl(20)	321.9 (4)
Cr···Cl(18)	340.6 (4)	Cr···Cl(24)	361.3 (4)
C(13)−C(14)	138.3(14)	C(19)−C(20)	140(2)
C(13)−C(18)	140(2)	C(19)−C(24)	138.6(15)
C(14)−Cl(14)	173.4(12)	C(20)−Cl(20)	175.0(11)
C(18)−Cl(18)	174.0(12)	C(24)−Cl(24)	172.0(12)
Cr-C(13)-C(14)	123.8(8)	Cr-C(19)-C(20)	116.1(8)
Cr-C(13)-C(18)	122.5(8)	Cr-C(19)-C(24)	128.8(9)
C(14)-C(13)-C(18)	113.7(10)	C(20)-C(19)-C(24)	114.9(11)
Coordination polyhedron		Cation	
C(1)-Cr-C(7)	111.7(4)	Li−O(1)	190(3)
C(1)-Cr-C(13)	94.2(4)	Li−O(2)	188(3)
C(1)-Cr-C(19)	141.5(4)	Li−O(3)	194(3)
C(1)-Cr-Cl(2)	59.5(3)	Li−O(4)	189(2)
C(1)-Cr-Cl(12)	83.1(3)	O(1)-Li-O(2)	112.0(13)
C(7)-Cr-C(13)	103.2(4)	O(1)-Li-O(3)	110.4(14)
C(7)-Cr-C(19)	90.8(4)	O(1)-Li-O(4)	104.1(13)
C(7)-Cr-Cl(2)	170.1(3)	O(2)-Li-O(3)	108.1(14)
C(7)-Cr-Cl(12)	63.2(3)	O(2)-Li-O(4)	117.2(15)
C(13)-Cr-C(19)	111.1(4)	O(3)-Li-O(4)	104.8(12)
C(13)-Cr-Cl(2)	74.2(3)		
C(13)-Cr-Cl(12)	163.4(3)		
C(19)-Cr-Cl(2)	99.0(3)		
C(19)-Cr-Cl(12)	79.8(4)		
Cl(2)-Cr-Cl(12)	117.4(1)		

[a] Shortest $Cr^{III}\cdots Cr^{III}$ distance = 1.04 nm.

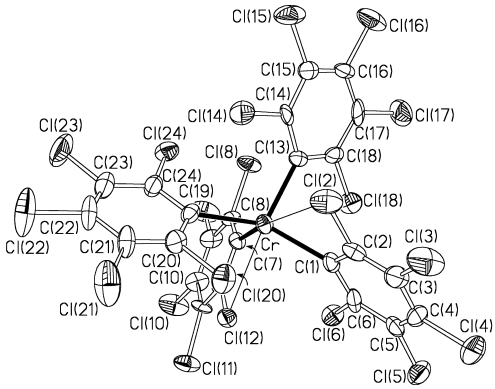

Figure 1. Thermal ellipsoid diagram (50% probability) of the anion of **1**.

small bite angle of the Cl_o-C_o-C_{ipso} unit, and 3) the fact that its two C atoms belong to a rigid phenyl ring, which should yield a very strained four-membered metallacycle. Despite all of these unfavorable factors, the chelating pentachlorophenyl-$\kappa C,\kappa Cl^2$ group in **1** is rather robust, since its formation is preferred over coordination of THF. In contrast, four THF molecules appear attached to the Li^+ ion, giving the commonly encountered tetrahedral complex cation $[Li(thf)_4]^+$.[23]

The small angles associated with the two four-membered metallacycles in the anion (C(1)-Cr-Cl(2) 59.5(3)° and C(7)-Cr-Cl(12) 63.2(3)°) introduce severe distortions in the overall geometry around the Cr^{III} center, which can be described as pseudo-octahedral. As a result, experimental values ranging from 74.2(3)° (C(13)-Cr-Cl(2)) to 117.4(1)° (Cl(2)-Cr-Cl(12)) are observed for the remaining angles involving *cis*-positioned atoms, instead of the ideal 90° angles. The angles associated with *trans*-positioned atoms also depart heavily from the expected 180° value (C(7)-Cr-Cl(2) 170.1(3)°, C(13)-Cr-Cl(12) 163.4(3)° and C(1)-Cr-C(19) 141.5(4)°).

Recently, a few pseudo-octahedral derivatives of platinum(IV)[24] and rhodium(III)[25, 26] (i.e., d^6 species) have been described, in which up to three pentachlorophenyl groups act as chelating ligands (Table 2). In each of these precedents as well as in **1**, the M−Cl interactions (M = Cr, Rh, Pt) involving pentachlorophenyl-$\kappa C,\kappa Cl^2$ groups are invariably located *trans* to a σ M−C bond. The related M−Cl distances are significantly longer than the mean values reported for the corresponding standard terminal $M-Cl_{term}$ bonds. This elongation can be associated with the formation of a highly strained four-membered metallacycle. The complex anion $[Rh^{III}\{C(O)C_6Cl_5\}_2(C_6Cl_5)Cl]^-$ provides unique experimental support for this assumption, since it contains three kinds of Rh−Cl interactions, each of them located *trans* to a C(sp^2) atom (acyl or aryl).[25] The terminal Rh−Cl bond has a normal length (239.3(1) pm) compared to the values reported for six-coordinate Rh^{III} compounds (mean value: 237.4 pm).[27] Remarkably, the Rh−Cl distance corresponding to the highly strained four-membered ring of the C_6Cl_5-$\kappa C,\kappa Cl^2$ ligand (288.6(1) pm) is much longer than that found for the five-membered ring of the $C(O)C_6Cl_5$-$\kappa C,\kappa Cl^2$ system (258.6(1) pm). The M−Cl distances in the anion $[Cr^{III}(C_6Cl_5)_4]^-$ are the longest described to date for this kind of interaction (281.8(3) and 300.1(4) pm) (Table 2), even though chromium is a first-row transition element.

Table 2. Structural data of the compounds containing the chelating pentachlorophenyl-$\kappa C,\kappa Cl^2$ ligand [bond lengths in pm].

Compound	$M-Cl_{short}$	$M-Cl_{long}$	mean value of $M-Cl_{term}$[a]	Ref.
$[Cr^{III}(C_6Cl_5)_4]^-$	281.8(3)	300.1(4)	233.5	this work
$[Pt^{IV}(C_6Cl_5)_4]$	255.9(2)	268.1(2)	232.6	[24]
$[Rh^{III}(C_6Cl_5)_4]^-$	262.8(1)	275.2(1)	237.4	[25]
$[Rh^{III}(C_6Cl_5)_3]$	258.9(2)	261.7(2)	237.4	[26a]
$[Rh^{III}(C_6Cl_5)_3Cl]^-$	265.6(4)	267.8(4)	237.4	[25]
$[Rh^{III}(C_6Cl_5)_3py]$[b]	260.2(9)	261.1(7)	237.4	[26b]
	255.7(7)	261.3(9)		
$[Rh^{III}(C_6Cl_4\text{-}C_6Cl_4)(C_6Cl_5)(tht)_2]$	286.8(1)		237.4	[26a]
$[Rh^{III}\{C(O)C_6Cl_5\}_2(C_6Cl_5)Cl]^-$	258.6(1)[c]	288.6(1)	237.4	[25]

[a] Values taken from ref. [27]. [b] The two sets of distances correspond to two crystallographically independent molecules within the crystal. [c] Distance corresponding to the $C(O)C_6Cl_5$ ligand.

We have also studied the redox behavior of complex **1** by electrochemical methods. Figure 2 shows the cyclic voltammogram (CV) of $[Cr^{III}(C_6Cl_5)_4]^-$ scanned at 100 mV s^{-1} from 0 to 1.6 to −1.6 and then back to 0 V. In the first part of the cycle, there is an oxidation wave ($(E_p)_{ox} = 0.82$ V), which is

 © 2002 WILEY-VCH Verlag GmbH & Co. KGaA, Weinheim 0947-6539/02/0817-4058 $ 20.00+.50/0 *Chem. Eur. J.* **2002**, *8*, No. 17

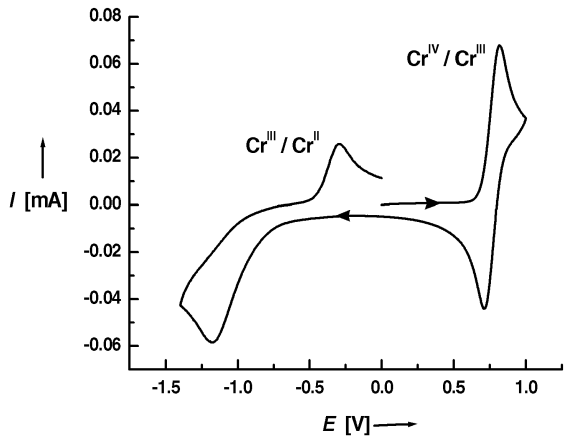

Figure 2. The CV of **1** in CH_2Cl_2 solution.

recovered in the returning scan ($(E_p)_{red} = 0.71$ V) corresponding to an electrochemically reversible semisystem ($E_{1/2} = 0.76$ V, $\Delta E_p = 0.11$ V, $i_{pa}/i_{pc} = 1.03$). At low potential another reduction wave is observed ($(E_p)_{red} = -1.18$ V), which is also recovered in the returning scan ($(E_p)_{ox} = -0.30$ V). The electrochemical correlation between these last waves has been checked to exist by means of a two-scan, partial CV measurement carried out in the low potential range (Figure 3). On scanning from -1.1 to 0 to -1.6 and then back to

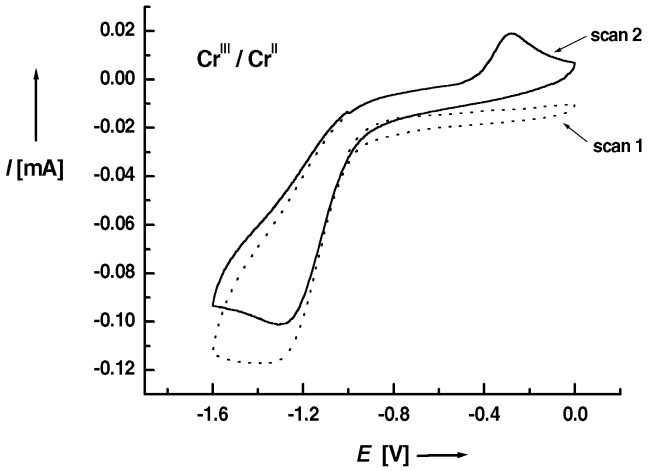

Figure 3. The CV of **1** at low potential (two scans; CH_2Cl_2 solution).

-1.1 V only the reduction wave at -1.18 V is observed. The fact that the oxidation wave at -0.30 V appears only in the second scan demonstrates that the two low-potential waves are electrochemically related. The very large peak-to-peak separation observed in this semisystem ($\Delta E_p = 0.88$ V) could be associated with a strong change in the geometry of the metal center. Redox-induced structural changes in any chemical species not implying the irreversible rupture of bonds are known to lead to moderate activation barriers during electron-transfer kinetics at electrode surface.[28] Specific cases of this general behavior are redox-induced isomeric interconversions such as *cis*/*trans* or *fac*/*mer* isomerization processes in mononuclear square-planar or octahedral metal complexes. However, there can also be more subtle structural changes, which involve the rearrangement of the ligands around the metal center leading to a different coordination polyhedron through the modification of bond lengths and angles.[24]

Considering that the two adjacent oxidation states II and IV are feasible for chromium, it is reasonable to assign the redox couples of the CV of **1** to each of the semisystems associated with the $Cr^{IV}/Cr^{III}/Cr^{II}$ sequence. To confirm this assumption we aimed to prepare and isolate all the chemical species involved in this redox system.

Synthesis of 2: All our attempts to oxidize **1** with Cl_2 dissolved in CCl_4 failed. Alternatively, we selected the salt $NOBF_4$ as a suitable oxidizing agent, considering its fairly high reduction potential (1.47 V vs SCE in CH_2Cl_2)[29] and the ease with which the reduced species, NO, can be removed from the reaction mixture. However, the 1:1.2 reaction of **1** with $NOBF_4$ gives only impure **2** in low yield (ca. 10%). The reaction was followed by IR and no evidence of the presence of coordinated nitrosyl was detected in solution. Better results were obtained using the radical aminium salt $[N(4\text{-}BrC_6H_4)_3][SbCl_6]$ (1.16 V vs SCE in CH_2Cl_2).[29] The 1:1.1 reaction of **1** with $[N(4\text{-}BrC_6H_4)_3][SbCl_6]$ gave analytically and spectroscopically pure $[Cr^{IV}(C_6Cl_5)_4]$ (**2**) in high yield (Scheme 1). Complex **2** is a brown solid of limited thermal stability, which has to be prepared, handled, and stored at low temperature (below 0 °C). It is scarcely soluble in most of the usual organic solvents and it gets reduced to $[Cr^{III}(C_6Cl_5)_4]^-$ when dissolved in THF. Saturated solutions of **2** in CH_2Cl_2 give a CV consistent with that described for complex **1**, but not so well resolved due to the low solubility of the sample.

The difficulty with which **1** is oxidized to **2** as well as the high potential required for the process are in sharp contrast with the reported behavior of homoleptic organoderivatives of the Cr^{IV}/Cr^{III} system. Thus, a number of neutral tetraorganylchromium(IV) derivatives have been prepared by reaction of $[CrCl_3(thf)_3]$ with the appropriate organylating agent (LiR or MgRX, in which $R = CH_2SiMe_3$,[30] CH_2CMe_3,[31] CH_2CMe_2Ph,[31] CH_2CPh_3,[31] 1-norbornyl,[32] 2,3,3-trimethylbicyclo[2.2.1]hetp-1-yl,[32] *t*Bu,[33] *c*-C_6H_{11}[34] or CPh=CMe_2[35]). The reactions have been suggested to proceed through formation of transient organochromium(III) species that have, in some instances, been detected but could not be isolated because they readily suffered oxidation giving the more stable neutral tetraorganylchromium(IV) derivatives. Even the compound $Li[Cr(2,4,6\text{-}Me_3C_6H_2)_4]\cdot 4THF$, obtained by treatment of $[Cr(2,4,6\text{-}Me_3C_6H_2)_3]\cdot THF$ with $Li(2,4,6\text{-}Me_3C_6H_2)$,[20] has been reported to be easily oxidized by air (oxygen) or Ph_3CCl to give the more stable and less reactive $[Cr(2,4,6\text{-}Me_3C_6H_2)_4]$.[36]

We have been unable to obtain suitable crystals of **2** for X-ray diffraction purposes. However, it is reasonable to assume a tetrahedral geometry as observed in the structurally characterized $[CrR_4]$ species ($R = CH_2CMe_2Ph$,[37] *c*-C_6H_{11},[34] CPh=CMe_2[35] or 2-methylen-3,3-dimethylbicyclo[2.2.1]hept-1-yl[38]). The magnetic properties of **2** are in agreement with this assumption (see below).

 © 2002 WILEY-VCH Verlag GmbH & Co. KGaA, Weinheim 0947-6539/02/0817-4059 $ 20.00+.50/0

Synthesis and structural characterization of 3: The reaction of $[CrCl_2(thf)]$ with LiC_6Cl_5 in 1:5 molar ratio followed by the appropriate treatment gives $[\{Li(thf)_3\}_2(\mu\text{-}Cl)]_2[Cr^{II}(C_6Cl_5)_4]$ (**3**) as an extremely air- and water-sensitive red solid in 47% yield (Scheme 1). Since it is also thermally labile, it must be prepared, stored, and handled under an inert atmosphere and at low temperature (below 0 °C).

The crystal structure of **3** has been established by X-ray diffraction methods. A selection of interatomic distances and angles is given in Table 3. The lattice is formed by the separate ions $[\{Li(thf)_3\}_2(\mu\text{-}Cl)]^+$ and $[Cr^{II}(C_6Cl_5)_4]^{2-}$ as shown in Figure 4. The cation contains two $\{Li(thf)_3\}^+$ units linked by a bridging chloride, which is located on a two-fold axis with an almost linear Li-Cl-Li core (174.2(6)°). The geometry around each of the Li^+ ions is roughly tetrahedral and the two Cl-bridged $[Li(thf)_3]^+$ units adopt a staggered conformation. All the distances and angles are virtually the same as those found in the only precedent known for this unusual cation, namely, $[\{Li(thf)_3\}_2(\mu\text{-}Cl)][\{ZrCp(\mu\text{-}PPh)\}_2]$.[39] The anion $[Cr^{II}(C_6Cl_5)_4]^{2-}$ can be described as a square-planar species, in which the Cr^{II} center is located at a four-fold axis and, hence, there is only one crystallographically independent C_6Cl_5 group per anion (Cr–C(1) 220.8(3) pm). In this case, all the C_6Cl_5 groups act as standard terminal σ-bonded ligands without any additional Cr–Cl_o interactions (cf. crystal structure of **1**). Accordingly, the two crystallographically independent *o*-Cl atoms are equidistant from the chromium(II) center (Cr···Cl(2) = Cr···Cl(6) = 345.2(1) pm) and the two Cr-C_{ipso}-C_o angles are virtually identical (Cr-C(1)-C(2) 123.6(3)° and Cr-C(1)-C(6) 123.2(3)°).

Table 3. Selected interatomic distances [pm] and angles [°] for **3**.[a]

Anion		Cation	
Cr–C(1)	220.8(3)	Li–O(1)	191.0(11)
Cr···Cl(2)	345.2(1)	Li–O(2)	195.0(11)
Cr···Cl(6)	345.2(1)	Li–O(3)	193.7(9)
C(1)–C(2)	139.3(5)	Li–Cl(7)	225.0(8)
C(1)–C(6)	140.0(5)	O(1)-Li-O(2)	106.0(4)
C(2)–Cl(2)	174.2(4)	O(1)-Li-O(3)	115.7(5)
C(6)–Cl(6)	174.3(4)	O(1)-Li-Cl(7)	109.4(5)
Cr-C(1)-C(2)	123.6(3)	O(3)-Li-O(2)	106.4(5)
Cr-C(1)-C(6)	123.2(3)	O(3)-Li-Cl(7)	108.2(4)
C(2)-C(1)-C(6)	113.3(3)	O(2)-Li-Cl(7)	111.1(4)
C(1)-Cr-C(1′)	89.999(3)	Li-Cl(7)-Li′	174.2(6)
C(1)-Cr-C(1″)	179.3(2)		
C(1)-Cr-C(1‴)	90.000(1)		
C(1′)-Cr-C(1″)	90.0		
C(1′)-Cr-C(1‴)	179.3(2)		
C(1″)-Cr-C(1‴)	89.997(1)		

[a] Shortest $Cr^{II}\cdots Cr^{II}$ distance = 1.47 nm.

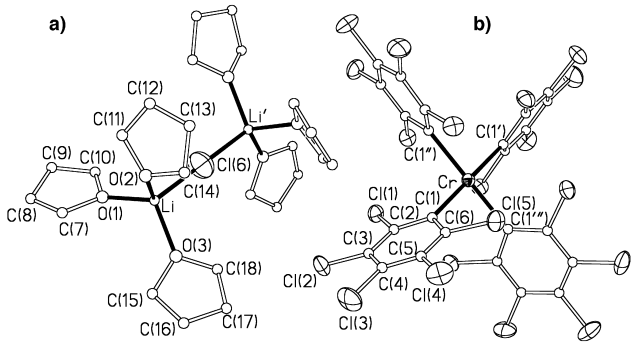

Figure 4. Thermal ellipsoid diagram (50% probability) of a) the cation and b) the anion of **3**.

A typical feature of Cr^{II} chemistry is the possibility of forming dinuclear species connected by a chromium-chromium quadruple bond. The existence of that high-order bond is certainly favored by the presence of efficient bridging ligands, since, in their absence, bond cleavage can be affected by secondary factors such as the nature of the cation/anion interaction. Thus, it has been reported recently that the quadruple bond in the dinuclear species $[Li(thf)]_4[Cr_2Me_8]$ is reversibly broken by mere replacement of THF by *N,N,N′,N′*-tetramethyl-1,2-ethanediamine (tmen) giving the paramagnetic, mononuclear derivative $[Li(tmen)]_2[CrMe_4]$.[40] In both of these compounds, the cation and the anion are associated through electron-deficient μ_2- or μ_3-methyl bridges. The relative acidity of the $[Li(solvent)]^+$ moiety (solvent = thf or tmen) seems to be an important factor affecting the cation/anion interaction and concomitantly the formation or breaking of the unsupported chromium–chromium quadruple bond. The presence of electron-deficient Cr-C-Li bridging systems is, in fact, a feature common to all the mononuclear tetraorganylchromate(II) derivatives, $[CrR_4]^{2-}$, for which the solid-state structure has been determined to date [R = Me,[40] Ph,[41] 2,4,6-$Me_3C_6H_2$[41] and $1/2(CH_2SiMe_2CH_2)$[42]]. It is therefore remarkable that cation and anion appear clearly separate in the crystals of **3**. The absence of any additional cation/anion interaction can be due to: 1) the low tendency of the C_6Cl_5 group to act as an electron-deficient bridging ligand[43] and 2) the reduced acidity of the cation $[\{Li(thf)_3\}_2(\mu\text{-}Cl)]^+$, which bears a single positive charge per Li_2 pair.

The electrochemical behavior of **3** is qualitatively similar to that observed for **1** and **2**. Moreover, **3** reacts with an equimolar amount of **2** giving **1** according to the following comproportionation scheme: $Cr^{II} + Cr^{IV} \rightarrow Cr^{III}$.

EPR measurements: The EPR spectra of compounds **1–3** are given in Figure 5. Cr^{II} and Cr^{IV} are non-Kramer systems

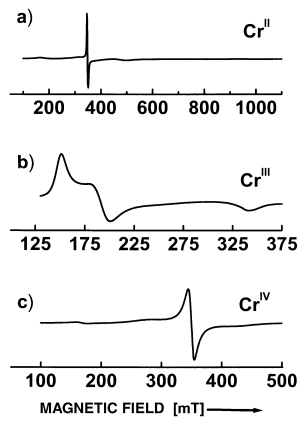

Figure 5. X-band EPR spectra of powder solid samples of compounds **1–3** at room temperature. Every spectrum was measured up to 1.5 T, but no additional signals were detected above the magnetic field indicated in each trace.

© 2002 WILEY-VCH Verlag GmbH & Co. KGaA, Weinheim
0947-6539/02/0817-4060 $ 20.00+.50/0 *Chem. Eur. J.* **2002**, *8*, No. 17

according to their even number of electrons, while Cr^{III} is a Kramer system with $S=3/2$. It is therefore advisable to analyze them separately.

The EPR spectrum of a powder sample of **1** (Figure 5b) is similar to that observed in a solution of frozen CH_2Cl_2,[12] but with a more pronounced orthorhombic behavior. Thus, the effective spin becomes $\tilde{\boldsymbol{S}}=1/2$ with the following spin Hamiltonian [Eq. (1)]:

$$H=\mu_B B(g'_x l_x \tilde{\boldsymbol{S}}_x + g'_y l_y \tilde{\boldsymbol{S}}_y + g'_z l_z \tilde{\boldsymbol{S}}_z) \quad (1)$$

in which $g'_x=4.377$, $g'_y=3.456$, and $g'_z=1.943$. As in the solution case,[12] the spectrum of the powder sample can be interpreted as being due to the $M=\pm 1/2$ transitions in the high zero-field splitting (ZFS) limit. In fact, no further transitions are detected up to 1.5 T and thus we can not estimate the ZFS parameters. Assuming, as in the solution case, an axial true $\tilde{\boldsymbol{g}}$ tensor for the isolated Cr^{III} ion and following the same procedure used there we obtain $g_{\parallel}=1.979$ and $g_{\perp}=1.967$ with $\eta=0.079\pm0.010$, η being the asymmetric parameter of the ZFS contribution. The g factor obtained following these assumptions is nearly isotropic, as is usually found in Cr^{III} complexes. Moreover, the deviation of these values from the free-electron g factor is also consistent with those previously reported for ionic[45] and coordination[46] Cr^{III} compounds.

Let us consider the case of the non-Kramers Cr^{II} and Cr^{IV} systems. The ground state of Cr^{IV} has a spin $S=1$. The EPR spectrum of **2** (Figure 5c) consists of a dominant isotropic line centered at about $g=1.980$ on a broader one together with a small signal at a field of about half strength. The EPR spectrum of **2** is closely related to those of Ni^{2+} species with $S=1$, which have been studied and analyzed in great detail.[47] The central broad feature, referred to as the normal line (NL), is associated with the $\Delta M=\pm 1$ transitions. The modulation of the splitting due to the crystal-field distribution accounts for the broadening of this line. The dominant, isotropic line at $g\approx 1.980$ can be ascribed to the $|+1\rangle \leftrightarrow |-1\rangle$ double quantum transition (DQL), which, in a first-order approximation, does not depend on the crystal field strength. The prominent DQL appears superimposed to the much broader NL. Moreover, the crystal field contribution makes the single quantum $|+1\rangle \leftrightarrow |-1\rangle$ transition partially allowed and thus a further signal appears in the "half field" region (HFL).

The EPR spectrum of **3** (Figure 5a) consists of a dominant narrow, almost isotropic line at about 348 mT ($g=1.99$) together with smaller and broader lines at approximately 190 and 480 mT. There are very few reports on EPR spectra of Cr^{II} ($S=2$) ions in the literature and they mainly correspond to isolated ions in ionic crystals,[48] semiconductors,[49] and, more recently, in aqueous solution.[50] In all these cases a spin $S=2$ has been found with an almost isotropic g factor, whose value is close to but lower than that of the free electron. The general spin Hamiltonian for an $S=2$ ion should contain the standard electronic Zeeman contribution as well as second- and fourth-range ZFS terms, and, hence, the observed transition should subtly depend on the orientation and strength of the high-order contributions. This difficulty precludes a detailed analysis of the spectrum given in Figure 5a and, therefore, an estimate of the ZFS parameters is not possible.

Magnetism measurements: A plot of magnetization per magnetic ion, expressed in Bohr magnetons ($M/N_A\mu_B$) against $\mu_0 H/T$ up to 5 T, at 1.8 K, for compounds **1–3** (Figure 6) clearly indicates the tendency to saturation. Taking a g factor close to that of the free electron value, a high-spin configuration is obtained for the metal ion in all three cases, that is, $S=2$, 3/2, and 1 for Cr^{II}, Cr^{III}, and Cr^{IV}, respectively.

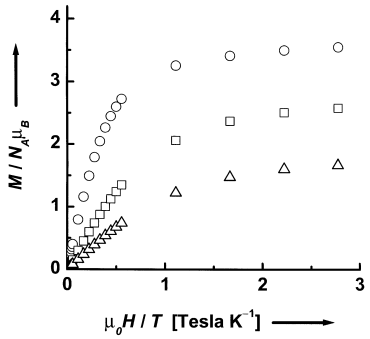

Figure 6. Magnetic-field dependence of the magnetization measured at low temperature (1.8 K) showing the saturation behavior. Cr^{II} (circles), Cr^{III} (squares), and Cr^{IV} (triangles).

In the low-field region ($\mu_0 H/T < 0.07\ \mathrm{T\,K^{-1}}$), linear dependencies are found for $M/N_A g\mu_B$ values against $\mu_0 H/T$ for the three samples **1–3** as shown in Figure 7. However, the slopes of the fitted straight lines depend to a slight extent on the

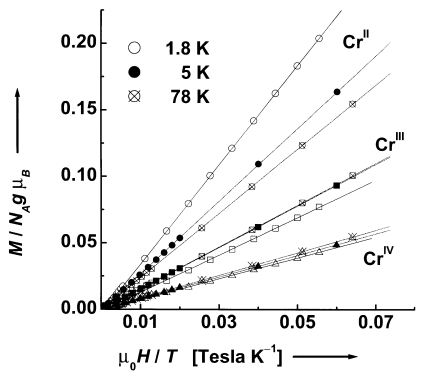

Figure 7. Dependence of the magnetization versus the applied magnetic field in the low-field region at 1.8 K (open symbols), 5 K (solid symbols), and 78 K (crossed symbols) for Cr^{II} (circles), Cr^{III} (squares), and Cr^{IV} (triangles). The lines correspond to a fitted linear dependence of the magnetization versus the quotient $\mu_0 H/T$ (see text).

temperature for each sample: they increase with the temperature for Cr^{III} and Cr^{IV}, while the opposite is observed for Cr^{II} (Figure 7). This behavior implies that the global magnetization data do not follow a Brillouin function and, accordingly, a simple Curie-law does not describe the thermal evolution of the magnetic susceptibility either. Linear relationships between $\chi(T)$ and $1/T$—as required by the Curie law—are observed *only* in the high-temperature region ($T>30$ K; Figure 8b). However, the fact that $\chi(T)$ versus $1/T$

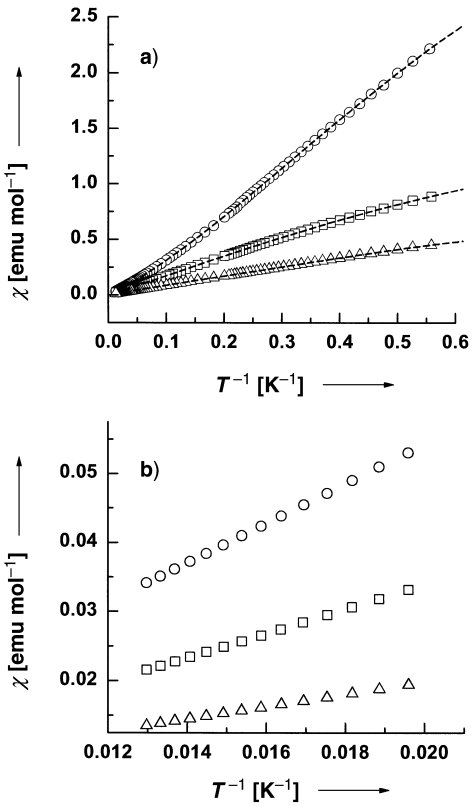

Figure 8. a) Magnetic susceptibility as a function of the inverse of the temperature for Cr^{II} (circles), Cr^{III} (squares), and Cr^{IV} (triangles) samples. The dotted lines represent the fitting of the data to the polynomial expansion given in Equation (2) up to the order indicated in Table 4. b) Detail of the high-temperature region ($T > 50$ K).

cannot be adjusted to simple linear functions in the whole temperature range[51] (Figure 8a) means that a different approach must be adopted.

In species containing a unique, non-interacting center with $S > 1/2$, as is the case of compounds **1**–**3**, the departure of the low-temperature magnetic data from a simple Curie law has been successfully ascribed to the zero-field splitting (ZFS) contribution.[51] Carlin and his co-workers have derived specific formulas to account for the thermal dependence of the anisotropic magnetic susceptibility in $S = 1$ ions as well as in $S = 3/2$ ions with axial symmetry.[51] These results, however, are of little use for our systems, since **1** is a Cr^{III} species ($S = 3/2$) with a clearly orthorhombic symmetry as revealed by its EPR spectrum (see above) and **3** is a Cr^{II} derivative with $S = 2$. Hence, we adopted a different approach by restricting to the situation in which the ZFS is comparatively lower than the thermal energy, kT, but high enough to induce a departure of the thermal dependence of the magnetic susceptibility from the Curie law. Starting with this premise, we derived a justification for the observed asymptotic temperature dependence of the magnetic susceptibility (see Supporting Information).

The temperature dependence of the magnetic susceptibility, $\chi(T)$, for the three organochromium compounds **1**–**3** has been analyzed over the whole temperature range measured ($1.8 < T < 78$ K) using solely the expression given in Equation (2), where C is the Curie constant, χ_0 includes the temperature independent (TIP) as well as the diamagnetic contribution, and the k_j ($j = 1, 2, \ldots$) constants contain information on the ZFS contribution.

$$\chi(T) = \chi_0 + \frac{C}{T}\left(1 + \frac{k_1}{T} + \frac{k_2}{T^2} + \ldots\right) \quad (2)$$

By fitting this expression to the experimental data (Figure 8), estimates of the Curie constant, C, as well as of the effective number of Bohr magnetons, p, and the experimental g values have been obtained for the three compounds (Table 4). It can be noted that the g value obtained from bulk magnetic measurements for the Cr^{III} compound **1** is in excellent agreement with that obtained from EPR results (see above).

Table 4. Parameters derived from magnetization measurements for compounds **1**–**3**.

	Polynomial order[a]	C [emu mol^{-1} K]	p [μ_B][b]	$g = \sqrt{\langle g^2 \rangle}$	$M/N_A g \mu_B$ (S) (5 T, 1.8 K)
Cr^{II}	3	2.85(3)	4.77(3)	1.95(1)	1.97 (2)
Cr^{III}	3	1.76(2)	3.75(3)	1.94(1)	1.33 (3/2)
Cr^{IV}	2	0.90(3)	2.68(3)	1.90(1)	0.88 (1)

[a] Order of the polynomial used to fit χ as a funtion of T^{-1} [see Eq. (2)].
[b] Magnetic moment per atom in Bohr magneton units.

The expression given in Equation (2) has been derived by using the basic microscopic magnetic properties of any system containing a unique magnetic center with ZFS contribution (see Supporting Information). In deriving this expression, it has been assumed that the ZFS contribution is small enough as to allow an asymptotic expansion of the temperature dependence of the magnetic susceptibility. Since no assumption about the kind of spin system has been made, this expression should be applicable to a wide variety of real systems.

Conclusion

The versatility of the pentachlorophenyl group has been confirmed in chromium chemistry as it has been possible to isolate and characterize a series of homoleptic organochromium derivatives in three adjacent oxidation states, Cr^{IV}, Cr^{III}, and Cr^{II}, with formula $[Cr(C_6Cl_5)_4]^{n-}$ ($n = 0$, 1, 2). This versatility is both electronic and steric, since the pentachlorophenyl group is not only able to stabilize different oxidation states on the same metal without the need for any further ancillary ligand, but also to accommodate to different geometric requirements imposed by the preferred coordination polyhedron adopted by the metal center in each case (Scheme 2). Thus, while the C_6Cl_5 group acts as a standard monodentate σ-organyl ligand in the square-planar Cr^{II} compound **3** as well as in the presumably tetrahedral Cr^{IV} species **2**, it is able to establish secondary interactions through one of the *ortho*-Cl atoms with the Cr^{III} center in complex **1** in order for this latter to achieve a (distorted) octahedral environment—by far the preferred geometry for Cr^{III}. In this case, the C_6Cl_5 group behaves as a small-bite chelating ligand.

 © 2002 WILEY-VCH Verlag GmbH & Co. KGaA, Weinheim 0947-6539/02/0817-4062 $ 20.00+.50/0 *Chem. Eur. J.* **2002**, *8*, No. 17

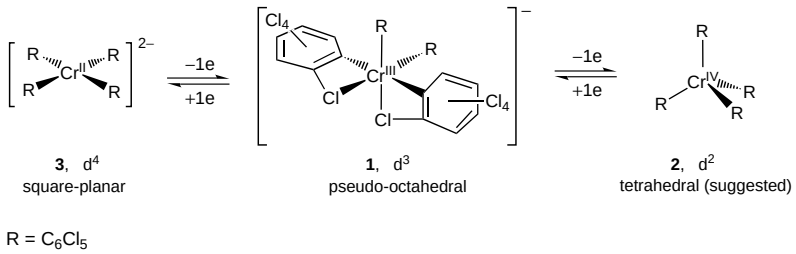

Scheme 2.

The only precedent for the isolation of a $[CrR_4]^{n-}$ series ($n = 0$, 1, 2) is found for $R = 2,4,6\text{-}Me_3C_6H_2$ (mesityl). This concomitance between the pentachlorophenyl and the mesityl groups is quite surprising, considering the disparity of the substituents on the phenyl ring, that is, Cl and CH_3, which bear very different inductive and resonance effects. It should be noted, however, that Cl and CH_3 substituents have been ascribed very similar steric demands as denoted by their assigned molecular van der Waals volume (0.0195 and 0.0222 nm^3, respectively).[52]

According to their magnetic behavior, the three compounds **1**–**3** are high-spin species with observable EPR spectra at room temperature. The temperature dependence of the magnetic susceptibility for the three species does not follow a simple Curie law, but a higher-order polynomial relationship [Eq. (2)], which can be derived from microscopic magnetic properties taking into account the zero-field splitting contribution (Supporting Information).

Experimental Section

General procedures and materials: All reactions and manipulations were carried out under purified argon using Schlenk techniques. Solvents were dried by standard methods and distilled prior to use. The chromium complexes $[CrCl_2(thf)]$[53] and $[CrCl_3(thf)_3]$,[54] as well as the organolithium reagent LiC_6Cl_5[55] were prepared as described elsewhere. The aminium salt $[N(4\text{-}BrC_6H_4)_3][SbCl_6]$ was purchased (Aldrich) and used as received. Elemental analyses were carried out with a Perkin–Elmer 2400-Series II microanalyzer. IR spectra of KBr discs were recorded on a Perkin–Elmer 883 spectrophotometer in the range 4000–200 cm^{-1}. Mass spectra were recorded on a VG-Autospec spectrometer using the standard Cs-ion FAB (acceleration voltage: 35 kV). Electrochemical studies were carried out using an EG&G model 273 potentiostat in conjunction with a three-electrode cell, in which the working electrode was a platinum disc, the auxiliary electrode a platinum wire, and the reference was an aqueous saturated calomel electrode (SCE) separated from the test solution by a fine-porosity frit and an agar bridge saturated with KCl. Where possible, solutions were 5×10^{-4} mol dm^{-3} in the test compound and 0.1 mol dm^{-3} in $[Nn Bu_4][PF_6]$ as the supporting electrolyte. At the end of each voltammetric experiment, $[Fe(\eta^5\text{-}C_5H_5)_2]$ was added to the solution as an internal standard for potential measurements. Under the conditions used, the E^o value for the couple $[Fe(\eta^5\text{-}C_5H_5)_2]^+/[Fe(\eta^5\text{-}C_5H_5)_2]$ was 0.47 V.

Synthesis of $[Li(thf)_4][Cr^{III}(C_6Cl_5)_4]$ (1): $[CrCl_3(thf)_3]$ (2.57 g, 6.85 mmol) was added to a solution of LiC_6Cl_5 (ca. 34 mmol) in Et_2O (130 mL) at −78 °C. The suspension was allowed to warm up to −10 °C and after about 4 h of stirring, the by then violet solid was filtered at 0 °C and extracted in CH_2Cl_2 (60 mL) at the same temperature. The solvent in the extract was replaced by THF (20 mL), and the slow diffusion of an *n*-hexane layer (60 mL) into it at −30 °C yielded **1** as violet crystals in 57% yield. Elemental analysis calcd (%) for $C_{40}H_{32}Cl_{20}CrLiO_4$: C 35.73, H 2.40; found: C 36.21, H 2.02; IR (KBr): $\tilde{\nu} = 1321$ (s), 1311 (s), 1281 (vs), 1219 (m), 1125 (m), 1059 (s), 1043 (vs; C-O-C_{asym}),[56] 915 (m), 887 (s; C-O-C_{sym}),[56] 822 (vs; C_6Cl_5: X-sensitive vibr.),[57] 667 (vs), 600 (w), 415 (m), 349 cm^{-1} (m); MS (FAB−): *m/z*: 1040 $[Cr(C_6Cl_5)_4]^-$, 828 $[Cr(C_6Cl_5)_3Cl]^-$, 793 $[Cr(C_6Cl_5)_3]^-$, 581 $[Cr(C_6Cl_5)_2Cl]^-$, 546 $[Cr(C_6Cl_5)_2]^-$.

Synthesis of $[Cr^{IV}(C_6Cl_5)_4]$ (2): The addition of a violet solution of **1** (0.49 g, 0.36 mmol) in CH_2Cl_2 (3 mL) at 0 °C to a deep blue solution of $[N(4\text{-}BrC_6H_4)_3][SbCl_6]$ (0.33 g, 0.40 mmol) in CH_2Cl_2 (5 mL) in an ice bath caused the immediate precipitation of a brown solid. After 15 min of stirring, the precipitate was filtered, washed with CH_2Cl_2 (80–100 mL) and dried in vacuo. The brown solid was identified as **2** (71% yield). Elemental analysis calcd (%) for $C_{24}Cl_{20}Cr$: C 27.47; found: C 27.41; IR (KBr): $\tilde{\nu} = 1397$ (s), 1336 (s), 1323 (vs), 1314 (vs), 1289 (vs), 1156 (s), 835 (s; C_6Cl_5: X-sensitive vibr.),[57] 681 (s), 615 (w), 563 (m), 348 (m), 264 cm^{-1} (s); MS (FAB−): *m/z*: 1040 $[Cr(C_6Cl_5)_4]^-$, 828 $[Cr(C_6Cl_5)_3Cl]^-$, 793 $[Cr(C_6Cl_5)_3]^-$.

Synthesis of $[\{Li(thf)_3\}_2(\mu\text{-}Cl)]_2[Cr^{II}(C_6Cl_5)_4]$ (3): $[CrCl_2(thf)]$ (1.39 g, 7.12 mmol) was added to a solution of LiC_6Cl_5 (ca. 36 mmol) in Et_2O (150 mL) at −78 °C. The suspension was allowed to warm up to −10 °C and after about 4 h of stirring, the by then salmon pink solid was filtered at 0 °C and extracted in CH_2Cl_2 (60 mL) at the same temperature. The solvent in the extract was replaced by THF (25 mL) and the slow diffusion of an Et_2O layer (60 mL) into it at −30 °C yielded **3** as red crystals in 47% yield. Elemental analysis calcd (%) for $C_{72}H_{96}Cl_{22}CrLi_4O_{12}$: C 42.95, H 4.80; found: C 41.78, H 4.57; IR (KBr): $\tilde{\nu} = 1307$ (vs), 1277 (s), 1226 (s), 1044 (vs; C-O-C_{asym}),[56] 915 (sh), 888 (s; C-O-C_{sym}),[56] 808 (s; C_6Cl_5: X-sensitive vibr.),[57] 658 cm^{-1} (s); MS (FAB−): *m/z*: 1040 $[Cr(C_6Cl_5)_4]^-$, 828 $[Cr(C_6Cl_5)_3Cl]^-$, 793 $[Cr(C_6Cl_5)_3]^-$, 581 $[Cr(C_6Cl_5)_2Cl]^-$, 546 $[Cr(C_6Cl_5)_2]^-$.

Comproportionation of 2 and 3: Compound **2** (0.18 g, 0.17 mmol) was added to a solution of **3** (0.28 g, 0.14 mmol) in CH_2Cl_2 (10 mL) at 0 °C, and the mixture was stirred for 90 min in an ice bath. During this time, the color of the reaction mixture changed from red to violet. Then the suspension was filtered to free it from unreacted **2**. The filtrate was concentrated to dryness and the resulting residue was redissolved in THF (2 mL). Subsequent addition of a layer of Et_2O (10 mL) and allowing the mixture to stand at −30 °C caused the crystallization of 0.173 g of a violet solid which was identified as **1** (46% yield).

X-ray structure determinations: Crystals of $\mathbf{1} \cdot 0.5\,Et_2O \cdot 0.5\,C_6H_{14}$ and **3** suitable for X-ray diffraction studies were carefully selected from the reaction bulk. Diffracted intensity data were taken from: a) crystals of $\mathbf{1} \cdot 0.5\,Et_2O \cdot 0.5\,C_6H_{14}$ mounted in lithium grease at the end of a glass fiber, and b) crystals of **3** mounted at the end of a quartz fiber and held in place with a fluorinated oil. Crystal data and related parameters are given in Table 5. For $\mathbf{1} \cdot 0.5\,Et_2O \cdot 0.5\,C_6H_{14}$, of the 10103 intensity data (other than checks) collected, 9956 unique observations remained after averaging of duplicate and equivalent measurements and deletion of systematic absences (R_{int} 0.089); of these, 4366 reflections had $I > 2\sigma(I)$; an absorption correction was applied based on 444 azimuthal scan data. For **3**, 16845 intensity data were collected from which 4237 unique observations remained after averaging of duplicate and equivalent measurements and deletion of systematic absences (R_{int} 0.0300), of which, 3860 relections had $I > 2\sigma(I)$; an absorption correction was applied based on 426 azimuthal scan data. Both structures were solved by Patterson and Fourier methods. All non-hydrogen atoms were refined anisotropically. H atoms were added at calculated positions (C–H = 96 pm) with isotropic displacement parameters assigned as 1.2 times the equivalent isotropic *U*'s of the corresponding C atoms. For the structure of $\mathbf{1} \cdot 0.5\,Et_2O \cdot 0.5\,C_6H_{14}$, the atoms of the crystallographically independent half *n*-hexane solvent molecule were refined with a common set of anisotropic thermal parameters and their C–C distances fixed to 154 pm. A final difference electron density map showed one peak above 1000 e nm^{-3} (max 1063; largest diff. hole −1053 e nm^{-3}) located very near the chromium atom. For the structure of **3**, a final difference electron density map showed no peaks above 1000 e nm^{-3} (max 886; largest diff. hole −274 e nm^{-3}). For both structures, full-matrix least-squares refinement of the models against F^2 converged to final residual indices given in Table 5. All calculations were carried out using the program SHELXL-93.[58] CCDC-174782 and CCDC-174783 contain the supplementary crystallographic data for this paper. These data

Table 5. Crystal data and structure refinement for $\mathbf{1}\cdot 0.5\,Et_2O\cdot 0.5\,C_6H_{14}$ and **3**.

	$\mathbf{1}\cdot 0.5\,Et_2O\cdot 0.5\,C_6H_{14}$	**3**
formula	$C_{45}H_{44}Cl_{20}CrLiO_{4.5}$	$C_{72}H_{96}Cl_{22}CrLi_4O_{12}$
M_r	1424.74	2013.15
T [K]	150(1)	150(1)
λ [pm]	71.073	71.073
crystal system	monoclinic	tetragonal
space group	$C2/c$	$I4$
a [pm]	4151.3(6)	1771.30(10)
b [pm]	1288.25(10)	1771.30(10)
c [pm]	2387.8(3)	1537.14(14)
β [°]	117.324(12)	90
V [nm^3]	11.345(3)	4.8228(6)
Z	8	2
ρ [g cm^{-3}]	1.668	1.386
μ [mm^{-1}]	1.187	0.779
$F(000)$	5736	2068
diffractometer	Enraf-Nonius CAD4	
2θ range [°]	4–50 $(+h, +k, \pm l)$	4–50 $(\pm h, \pm k, \pm l)$
final R indices $[I>2\sigma(I)]$[a]	$R_1=0.0870$, $wR_2=0.1654$	$R_1=0.0416$, $wR_2=0.1189$
R indices (all data)	$R_1=0.2433$, $wR_2=0.2324$	$R_1=0.0502$, $wR_2=0.1608$
goodness-of-fit on F^2[b]	1.037	1.095
abs. structure parameter	–	0.00(4)

[a] $R_1=\Sigma(|F_o|-|F_c|)/\Sigma|F_o|$; $wR_2=[\Sigma w(F_o^2-F_c^2)^2/\Sigma w(F_c^2)^2]^{1/2}$; $w=[\sigma^2(F_o^2)+(g_1P)^2+g_2P]^{-1}$; $P=(1/3)\cdot[\max\{F_o^2,0\}+2F_c^2]$. [b] Goodness-of-fit $=[\Sigma w(F_o^2-F_c^2)^2/(n_{obs}-n_{param})]^{1/2}$.

can be obtained free of charge via www.ccdc.cam.ac.uk/conts/retrieving.html (or from the Cambridge Crystallographic Data Centre, 12, Union Road, Cambridge CB2 1EZ, UK; fax: (+44) 1223-336-033; or deposit@ccdc.cam.ac.uk).

Magnetic studies: Magnetic measurements were performed in a commercial SQUID magnetometer. Isothermal dc magnetization curves, $M(\mu_0H)$, at $T=1.8$, 5 and 78 K were taken for the three compounds, in the magnetic field range $0<\mu_0H<5$ T. As expected,[51] linear dependencies in $M(\mu_0H)$ were found at low fields (i.e., $g\mu_0H/k_BT<0.1$ or $\mu_0H/T<0.07$ T K^{-1}). Thus, to determine the thermal evolution of the magnetic susceptibility, $\chi(T)$, as the quotient $M(T)/\mu_0H$, a constant magnetic field value of $\mu_0H=0.1$ T, well within the linear regime for this temperature range, was used. Under that field $M(T)$ was measured for each compound in the temperature range $1.8<T<78$ K.

EPR measurements: EPR data were taken in a Varian E-112 or in a Bruker ESP380 spectrometer. The magnetic field was measured with a Bruker ER035M gaussmeter. A Hewlett–Packard HP5350B frequency counter was used to determine the microwave frequency.

Acknowledgements

We thank the Dirección General de Enseñanza Superior (Projects PB98–1595-C02-01 and PB98-1593) for financial support and the Gobierno de Aragón for a grant to M. A. G.-M. We also thank Dr. José M. Casas (University of Zaragoza) and Prof. Dr. Neil G. Connelly (University of Bristol) for invaluable help in the electrochemical measurements as well as in the analysis of the data obtained.

[1] Early reports: a) J. Sand, F. Singer, *Liebigs Ann. Chem.* **1903**, *329*, 190–194; b) G. M. Bennett, E. E. Turner, *J. Chem. Soc.* **1914**, 1057–1062.
[2] F. Hein, *Ber. Dtsch. chem. Ges.* **1919**, *52*, 195–196; F. Hein, *Ber. Dtsch. chem. Ges.* **1921**, *54*, 1905–1938; references to further reports on polyphenylchromium derivatives by Hein and co-workers are given in ref. [3].
[3] F. A. Cotton, *Chem. Rev.* **1955**, *55*, 551–594.
[4] H. H. Zeiss, M. Tsutsui, *J. Am. Chem. Soc.* **1957**, *79*, 3062–3066; see also ref. [3].
[5] E. O. Fischer, W. Hafner, *Z. Naturforsch. Teil B* **1955**, *10*, 665–668; E. O. Fischer, D. Seus, *Chem. Ber.* **1956**, *89*, 1809–1815.
[6] E. Uhlig, *Organometallics* **1993**, *12*, 4751–4756.
[7] R. Davis, L. A. P. Kane-Maguire in *Comprehensive Organometallic Chemistry*, *Vol. 3* (Eds.: G. Wilkinson, F. G. A. Stone, E. W. Abel), Pergamon, Oxford (UK), **1982**, Section 26.2, pp. 953–1077; M. J. Morris, in *Comprehensive Organometallic Chemistry II*, *Vol. 5* (Eds.: E. W. Abel, F. G. A. Stone, G. Wilkinson), Elsevier Science, Oxford (UK), **1995**, Chapter 8, pp. 471–549.
[8] The term "homoleptic" appears as a generalization of the older and useful concept of "binary" compound. It was first introduced by Lappert: P. J. Davidson, M. F. Lappert, R. Pearce, *Chem. Rev.* **1976**, *76*, 219–242.
[9] S. W. Kirtley in *Comprehensive Organometallic Chemistry*, *Vol. 3* (Eds.: G. Wilkinson, F. G. A. Stone, E. W. Abel), Pergamon, Oxford (UK), **1982**, Chapter 26.1, pp. 783–951; M. J. Winter, S. Woodward in *Comprehensive Organometallic Chemistry II*, *Vol. 5* (Eds.: E. W. Abel, F. G. A. Stone, G. Wilkinson), Elsevier Science, Oxford (UK), **1995**, Chapter 5, pp. 281–329; S. U. Koschmieder, G. Wilkinson, *Polyhedron* **1991**, *10*, 135–173; R. R. Schrock, G. W. Parshall, *Chem. Rev.* **1976**, *76*, 243–268; see also ref. [8].
[10] A. Fürstner, *Chem. Rev.* **1999**, *99*, 991–1045; L. A. Wessjohann, G. Scheid, *Synthesis* **1999**, 1–36.
[11] K. H. Theopold, *Eur. J. Inorg. Chem.* **1998**, 15–24; P. W. Jolly, *Acc. Chem. Res.* **1996**, *29*, 544–551; K. H. Theopold, *Acc. Chem. Res.* **1990**, *23*, 263–270.
[12] P. J. Alonso, L. R. Falvello, J. Forniés, M. A. García-Monforte, A. Martín, B. Menjón, G. Rodríguez, *Chem. Commun.* **1998**, 1721–1722.
[13] W. Herwig, H. H. Zeiss, *J. Am. Chem. Soc.* **1957**, *79*, 6561; W. Herwig, H. H. Zeiss, *J. Am. Chem. Soc.* **1959**, *81*, 4798–4801.
[14] M. M. Olmstead, P. P. Power, S. C. Shoner, *Organometallics* **1988**, *7*, 1380–1385; F. Hein, R. Weiss, *Z. Anorg. Allg. Chem.* **1958**, *295*, 145–152.
[15] J. Krause, G. Marx, *J. Organomet. Chem.* **1974**, *65*, 215–222; E. Kurras, J. Otto, *J. Organomet. Chem.* **1965**, *4*, 114–118.
[16] F. A. Cotton, G. Wilkinson, C. A. Murillo, M. Bochman, *Advanced Inorganic Chemistry*, 6th. ed., Wiley, New York, **1999**, Section 17-C-4, pp. 744–749; L. F. Larkworthy, K. B. Nolan, P. O'Brien, in *Comprehensive Coordination Chemistry*, *Vol. 3* (Eds.: G. Wilkinson, R. D. Gillard, J. A. McCleverty), Pergamon, Oxford (UK), **1987**, Section 35.4, pp. 772–927.
[17] E. Müller, J. Krause, K. Schmiedeknecht, *J. Organomet. Chem.* **1972**, *44*, 127–140; F. Hein, K. Schmiedeknecht, *J. Organomet. Chem.* **1966**, *5*, 454–462.
[18] G. K. Barker, M. F. Lappert, J. A. K. Howard, *J. Chem. Soc. Dalton Trans.* **1978**, 734–740.
[19] F. Hein, D. Tille, *Z. Anorg. Allg. Chem.* **1964**, *329*, 72–82.
[20] W. Seidel, G. Kreisel, *Z. Anorg. Allg. Chem.* **1976**, *426*, 150–154.
[21] F. Hein, K. Schmiedeknecht, *J. Organomet. Chem.* **1967**, *8*, 503–509.
[22] See however: R. J. Kulawiec, R. H. Crabtree, *Coord. Chem. Rev.* **1990**, *99*, 89–115.
[23] W. N. Setzer, P. von R. Schleyer, *Adv. Organomet. Chem.* **1985**, *24*, 353–451.
[24] J. Forniés, B. Menjón, R. M. Sanz-Carrillo, M. Tomás, N. G. Connelly, J. G. Crossley, A. G. Orpen, *J. Am. Chem. Soc.* **1995**, *117*, 4295–4304.
[25] M. P. García, M. V. Jiménez, A. Cuesta, C. Siurana, L. A. Oro, F. J. Lahoz, J. A. López, M. P. Catalán, A. Tiripicchio, M. Lanfranchi, *Organometallics* **1997**, *16*, 1026–1036.
[26] a) M. P. García, M. V. Jiménez, F. J. Lahoz, J. A. López, L. A. Oro, *J. Chem. Soc. Dalton Trans.* **1998**, 4211–4214; b) M. P. García, A. P. Martínez, M. V. Jiménez, C. Siurana, L. A. Oro, F. J. Lahoz, A. Tiripicchio, *Inorg. Chim. Acta* **2000**, *308*, 51–58.
[27] A. G. Orpen, L. Brammer, F. H. Allen, O. Kennard, D. G. Watson, R. Taylor, *J. Chem. Soc. Dalton Trans.* **1989**, S1–S83.
[28] W. E. Geiger, *Progr. Inorg. Chem.* **1985**, *33*, 275–352.
[29] N. G. Connelly, W. E. Geiger, *Chem. Rev.* **1996**, *96*, 877–910; the reduction potentials for the species NO^+ and $[N(4\text{-}BrC_6H_4)_3]^+$ were originally given versus the couple $[Fe(\eta^5\text{-}C_5H_5)_2]^+/[Fe(\eta^5\text{-}C_5H_5)_2]$. These values appear modified versus SCE in the text.
[30] W. Mowat, A. Shortland, G. Yagupsky, N. J. Hill, M. Yagupsky, G. Wilkinson, *J. Chem. Soc. Dalton Trans.* **1972**, 533–542; G. Yagupsky,

 © 2002 WILEY-VCH Verlag GmbH & Co. KGaA, Weinheim

W. Mowat, A. Shortland, G. Wilkinson, *J. Chem. Soc. Chem. Commun.* **1970**, 1369–1370.
[31] W. Mowat, A. J. Shortland, N. J. Hill, G. Wilkinson, *J. Chem. Soc. Dalton Trans.* **1973**, 770–778; W. Mowat, G. Wilkinson, *J. Organomet. Chem.* **1972**, *38*, C35-C36.
[32] B. K. Bower, H. G. Tennent, *J. Am. Chem. Soc.* **1972**, *94*, 2512–2514.
[33] W. Kruse, *J. Organomet. Chem.* **1972**, *42*, C39–C42.
[34] P. Stavropoulos, P. D. Savage, R. P. Tooze, G. Wilkinson, B. Hussain, M. Motevalli, M. B. Hursthouse, *J. Chem. Soc. Dalton Trans.* **1987**, 557–562.
[35] C. J. Cardin, D. J. Cardin, J. M. Kelly, R. J. Norton, A. Roy, B. J. Hathaway, T. J. King, *J. Chem. Soc. Dalton Trans.* **1983**, 671–677; C. J. Cardin, D. J. Cardin, A. Roy, *J. Chem. Soc. Chem. Commun.* **1978**, 899–900.
[36] W. Seidel, I. Bürger, *Z. Anorg. Allg. Chem.* **1976**, *426*, 155–158.
[37] V. Gramlich, K. Pfefferkorn, *J. Organomet. Chem.* **1973**, *61*, 247–248.
[38] G. G. Aleksandrov, I. V. Shchirina-Eingorn, I. I. Kritskaya, Yu. T. Struchkov, *Koord. Khim.* **1981**, *7*, 761–764.
[39] T. A. Bazhenova, A. V. Kulikov, A. F. Shestakov, A. E. Shilov, M. Yu. Antipin, K. A. Lyssenko, Yu. T. Struchkov, V. D. Makhaev, *J. Am. Chem. Soc.* **1995**, *117*, 12176–12180.
[40] S. Hao, J.-I. Song, P. Berno, S. Gambarotta, *Organometallics* **1994**, *13*, 1326–1335; S. Hao, S. Gambarotta, C. Bensimon, *J. Am. Chem. Soc.* **1992**, *114*, 3556–3557.
[41] J. J. H. Edema, S. Gambarotta, F. van Bolhuis, W. J. J. Smeets, A. L. Spek, M. Y. Chiang, *J. Organomet. Chem.* **1990**, *389*, 47–59.
[42] P. M. Morse, M. D. Spencer, S. R. Wilson, G. S. Girolami, *Organometallics* **1994**, *13*, 1646–1655.
[43] Alkyl and aryl groups acting as electron-deficient bridging ligands is a well documented phenomenon. Even the highly electron-withdrawing C_6F_5 group has been recently found to be suited to this role (see ref. [44]). However, to our knowledge, no bridging C_6Cl_5 group has been yet reported.
[44] J. M. Casas, J. Forniés, A. Martín, B. Menjón, M. Tomás, *Polyhedron* **1996**, *15*, 3599–3604; R. Usón, J. Forniés, L. R. Falvello, M. Tomás, J. M. Casas, A. Martín, F. A. Cotton, *J. Am. Chem. Soc.* **1994**, *116*, 7160–7165; R. Usón, J. Forniés, M. Tomás, J. M. Casas, F. A. Cotton, L. R. Falvello, X. Feng, *J. Am. Chem. Soc.* **1993**, *115*, 4145–4154; R. Usón, J. Forniés, M. Tomás, J. M. Casas, R. Navarro, *J. Chem. Soc. Dalton Trans.* **1989**, 169–172; R. Usón, J. Forniés, M. Tomás, J. M. Casas, F. A. Cotton, L. R. Falvello, R. Llusar, *Organometallics* **1988**, *7*, 2279–2285.
[45] P. J. Alonso, R. Alcalá, J. Casas-González, R. Cases, V. M. Orera, *J. Phys. Chem. Solids* **1989**, *50*, 1185–1191; R. Alcalá, P. J. Alonso, V. M. Orera, H. W. den Hartog, *Phys. Rev. B* **1985**, *32*, 4158–4163; R. W. Therhune, J. Lambe, C. Kikuchi, J. Baker, *Phys. Rev.* **1961**, *123*, 1265–1268; J. E. Wertz, P. Auzins, *Phys. Rev.* **1957**, *106*, 484–488; J. M. Baker, B. Bleaney, K. D. Browers, *Proc. Phys. Soc. London Sect. B* **1956**, *69*, 1205–1215.
[46] K. K. Narang, V. P. Singh, D. Bhattacharya, *Synth. React. Inorg. Met.-Org. Chem.* **1998**, *28*, 37–49; F. H. Köhler, B. Metz, W. Strauss, *Inorg. Chem.* **1995**, *34*, 4402–4413; B. S. Garg, R. K. Garg, M. J. Reddy, *J. Coord. Chem.* **1994**, *33*, 109–116; A. R. Oki, H. Zhang, J. A. Maguire, N. S. Hosmane, H. Ro, W. E. Hatfield, M. Moscherosch, W. Kaim, *Organometallics* **1992**, *11*, 4202–4213; U. Casellato, R. Graziani, R. P. Bonomo, A. J. Di Bilio, *J. Chem. Soc. Dalton Trans.* **1991**, 23–31.
[47] B. Villacampa, R. Alcalá, P. J. Alonso, J. M. Spaeth, *J. Phys. Condens. Matter* **1993**, *5*, 747–756; P. J. Alonso, R. Alcalá, J. M. Spaeth, *Phys. Rev. B* **1990**, *41*, 10902–10905.
[48] P. B. Oliete, V. M. Orera, P. J. Alonso, *Phys Rev. B* **1996**, *54*, 12099–12108; P. B. Oliete, V. M. Orera, P. J. Alonso, *Phys Rev. B* **1996**, *53*, 3047–3054; P. B. Oliete, V. M. Orera, P. J. Alonso, *J. Phys. Condens. Matter* **1996**, *8*, 7179–7190; M. M. Zaripov, V. F. Tarasov, V. A. Ulanov, G. S. Shakurov, *Phys. Solid State* **1996**, *38*, 249–252; M. M. Zaripov, V. F. Tarasov, V. A. Ulanov, G. S. Shakurov, M. L. Popov, *Phys. Solid State* **1995**, *37*, 437–440; P. B. Oliete, V. M. Orera, P. J. Alonso, *Radiat. Eff. Defects Solids* **1995**, *135*, 179–182.
[49] G. H. Stauss, J. J. Krebs, R. L. Henry, *Phys Rev. B* **1977**, *16*, 974–977; J. J. Krebs, G. H. Stauss, *Phys Rev. B* **1977**, *16*, 971–973; J. T. Vallin, G. D. Watkins, *Phys Rev. B* **1974**, *9*, 2051–2072.
[50] J. Telser, L. A. Pardi, J. Krzystek, L.-C. Brunel, *Inorg. Chem.* **1998**, *37*, 5769–5775.
[51] R. L. Carlin, *Magnetochemistry*, Springer, Berlin (Germany), **1986**.
[52] A. Gavezzotti in *Structure Correlation*, *Vol. 2* (Eds.: H.-B. Bürgi, J. D. Dunitz), VCH, Weinheim (Germany), **1994**, Chapter 12, pp. 509–542.
[53] F. H. Köhler, W. Prössdorf, *Z. Naturforsch. Teil B* **1977**, *32*, 1026–1029.
[54] P. Boudjouk, J.-H. So in *Inorganic Syntheses*, *Vol. 29* (Ed.: R. N. Grimes), Wiley, New York, **1992**, pp. 108–111.
[55] M. D. Rausch, F. E. Tibbets, H. B. Gordon, *J. Organomet. Chem.* **1966**, *5*, 493–500.
[56] G. M. Barrow, S. Searles, *J. Am. Chem. Soc.* **1953**, *75*, 1175–1177; L. J. Bellamy, *The Infra-Red Spectra of Complex Molecules*, *Vol. 1*, 3rd ed., Chapman and Hall, London (UK), **1975**, Chapter 7, pp. 129–140.
[57] R. Usón, J. Forniés, *Adv. Organomet. Chem.* **1988**, *28*, 219–297; E. Maslowsky, Jr., *Vibrational Spectra of Organometallic Compounds*, Wiley, New York, **1977**, pp. 437–442.
[58] G. M. Sheldrick, SHELXL-93, Program for the Refinement of Crystal Structures from Diffraction Data, University of Göttingen, Göttingen (Germany), **1993**.

Received: December 3, 2001
Revised: May 3, 2002 [F3715]

 © 2002 WILEY-VCH Verlag GmbH & Co. KGaA, Weinheim 0947-6539/02/0817-4065 $ 20.00+.50/0